CHEMISTRY OF MATERIALS

Article

pubs.acs.org/cm

Pressure Effect on Intersite Charge Transfer in A-site-Ordered Double-Perovskite-Structure Oxide

You-wen Long,[†,‡] Takateru Kawakami,[§] Wei-tin Chen,[†] Takashi Saito,[†] Tetsu Watanuki,[∥] Yuta Nakakura,[§] Qing-qing Liu,[‡] Chang-qing Jin,[‡] and Yuichi Shimakawa*[,†,⊥]

[†]Institute for Chemical Research, Kyoto University, Uji, Kyoto 611-0011, Japan

[‡]Beijing National Laboratory for Condensed Matter Physics, Institute of Physics, Chinese Academy of Sciences, Beijing 100190, China

[§]Institute of Quantum Science, Nihon University, Chiyoda, Tokyo 101-8308, Japan

[∥]Condensed Matter Science Division, Japan Atomic Energy Agency, 1-1-1 Kouto, Sayo, Hyogo 679-5148, Japan

[⊥]Japan Science and Technology Agency, CREST, Uji, Kyoto 611-0011, Japan.

ABSTRACT: The intersite charge transfer at room temperature was found to occur by applying pressure in the A-site-ordered double-perovskite-structure oxide $LaCu_3Fe_4O_{12}$. The pressure-induced charge transfer between the A-site Cu and B-site Fe causes a first-order-type transition from low-pressure $LaCu^{3+}{}_3Fe^{3+}{}_4O_{12}$ to high-pressure $LaCu^{2+}{}_3Fe^{3.75+}{}_4O_{12}$. The transition is accompanied by significant reduction of unit-cell volume, by unusual softening in bulk modulus, and by a change from an antiferromagnetic-and-insulating state to a paramagnetic-and-metallic state. The intersite charge-transfer transition in $LaCu_3Fe_4O_{12}$ is induced by changing pressure at ambient temperature as well as by changing temperature at ambient pressure. Besides, either physical pressure or chemical pressure, which is induced by cation substitution at the A′ site, decreases the intersite charge-transfer transition temperature, and reducing the unit-cell volume stabilizes Cu^{2+} at the A site and unusual high-valence $Fe^{3.75+}$ at the B site in the A-site-ordered double-perovskite-structure oxides.

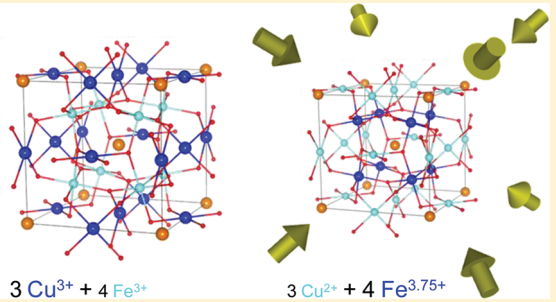

KEYWORDS: *pressure effect, double-perovskite-structure oxides, intersite charge transfer, unusual high-valence state*

1. INTRODUCTION

Perovskite-structure oxides, with the general formula ABO_3, usually contain alkaline metal, alkaline-earth metal, and lanthanide ions at the A site. An A-site-ordered double perovskite structure with the chemical formula $A'A_3B_4O_{12}$ can be formed by substituting a transition-metal ion such as Cu^{2+} or Mn^{3+} for 3/4 of the A-site ions in a simple ABO_3 perovskite.[1,2] This ordered perovskite usually has a cubic crystal structure with a space group $Im\bar{3}$ with A′ ions at the 2*a* (0, 0, 0), A ions at the 6*b* (0, 0.5, 0.5), B ions at the 8*c* (0.25, 0.25, 0.25), and oxygen ions at the 24*g* (*x*, *y*, 0) positions, as shown in Figure 1. In this structure the BO_6 octahedron is rigid but significantly tilted, giving rise to a square-coordinated AO_4 unit. From a structural point of view, the flexibility for tilting the BO_6 octahedra in $A'A_3B_4O_{12}$ is rather limited because of the need to maintain the square-planar coordination at the originally 12-fold-coordinated A site in the simple perovskite structure. Thus, high-pressure synthesis is often useful to stabilize such a crystal structure.

Because both the A and B sites in $A'A_3B_4O_{12}$ can accommodate transition-metal ions, materials with this structure often exhibit intriguing properties due to A−B intersite interaction as well as A−A and B−B interactions.[3−5] For instance, a ferrimagnetic transition above room temperature was observed in $CaCu_3Mn_4O_{12}$ due to the antiferromagnetic coupling between the spins at A-site Cu and B-site Mn.[6,7] Substitution of trivalent La or Bi for the divalent Ca in

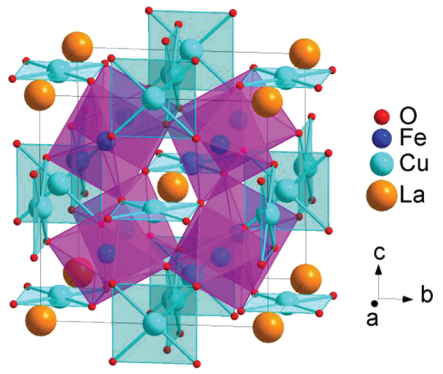

Figure 1. Crystal structure of A-site-ordered double-perovskite-structure oxide $LaCu_3Fe_4O_{12}$. The Cu ions at the A site make the square-planar AO_4 units and the Fe ions at the B site form corner-sharing BO_6 octahedra.

Received: April 25, 2012
Published: May 14, 2012

$CaCu_3Mn_4O_{12}$ induced valence mixing in the B-site Mn and gave $(La/Bi)Cu_3Mn_4O_{12}$ a half-metallic nature with spin-polarized conduction carriers, leading to a large magneto-resistance effect.[8−10]

Another phenomenon caused by the A-B intersite interaction in the A-site-ordered double-perovskite-structure oxide $LaCu_3Fe_4O_{12}$ was recently found; temperature-induced charge transfer.[11] The compound was synthesized under a high-pressure and high-temperature condition. At room temperature the charge formula of the compound was $LaCu^{3+}{}_3Fe^{3+}{}_4O_{12}$, where an unusual Cu^{3+} valence state at the square-planar-coordinated A site was stabilized. Heating induced the charge transfer at 393 K from the B-site Fe ions to the A-site Cu ions ($4Fe^{3+} - 3e^- \rightarrow 4Fe^{3.75+}$ and $3Cu^{3+} + 3e^- \rightarrow 3Cu^{2+}$) and the charge formula changed to $LaCu^{2+}{}_3Fe^{3.75+}{}_4O_{12}$. The high-temperature phase contained irons in the unusually high valence state $Fe^{3.75+}$. The transition did not change the crystal-structure symmetry but drastically changed the unit-cell volume, leading to a negative-thermal-expansion-like volume contraction. This intersite charge transfer also associated with antiferromagnetism-to-paramagnetism and insulator-to-metal transitions.[12]

Like temperature, pressure can also modify the valence states of transition-metal ions in oxides. It is thus interesting to examine the effect of pressure on the intersite charge-transfer transition in $LaCu_3Fe_4O_{12}$ without changing the temperature. In this study, we measured the synchrotron X-ray diffraction (SXRD), Mössbauer spectra, and electric transport of $LaCu_3Fe_4O_{12}$ at room temperature and under high pressures ranging from ambient pressure to about 8 GPa. We found that pressure decreased the intersite charge-transfer transition temperature and induced the charge change between the A-site Cu and B-site Fe ions in $LaCu_3Fe_4O_{12}$ at room temperature. The observed physical pressure effect is also discussed with comparison of chemical pressure effect induced by the cation substitution.

2. EXPERIMENTAL SECTION

$LaCu_3Fe_4O_{12}$ was prepared by a solid-state reaction at 10 GPa and 1400 K in a way described in a previous report.[11] A cubic anvil-type high-pressure apparatus was used for the reaction. The starting materials were La_2O_3, CuO and Fe_2O_3, and $KClO_4$ was used as an oxidizing agent. The sample synthesized was confirmed to be a single phase with the A-site-ordered double perovskite structure. No anomalies in the occupation factors for any sites were observed in the structure refinements, indicating that the compound had the stoichiometric composition.

The preliminary high-pressure SXRD experiment was done at the Beijing Synchrotron Radiation Facility. The detailed diffraction experiment was done at beamline BL22XU in SPring-8 by using a diamond anvil cell (DAC) with a stainless-steel gasket. A mixture of methanol and ethanol with a molar ratio of 4:1 was used as a pressure-transmitting medium in the DAC, and the applied pressure was calibrated using the ruby fluorescence method.[13] The wavelength used in the detailed experiment was 0.49613 Å. The GSAS Rietveld program was used to analyze the SXRD data.[14]

The high-pressure ^{57}Fe Mössbauer spectra were obtained on a Basset-type DAC with a Re gasket. ^{57}Co in Rh and a control absorber consisting of α-Fe were used. Daphne 7474 was used as a pressure-transmitting medium. The resistivity under pressure was measured using a four-probe method with a cubic-anvil-type high-pressure apparatus. All the measurements were made at room temperature.

3. RESULTS AND DISCUSSION

Figure 2a shows the pressure dependence of SXRD patterns. The structure analysis from the diffraction data at 0.3 GPa

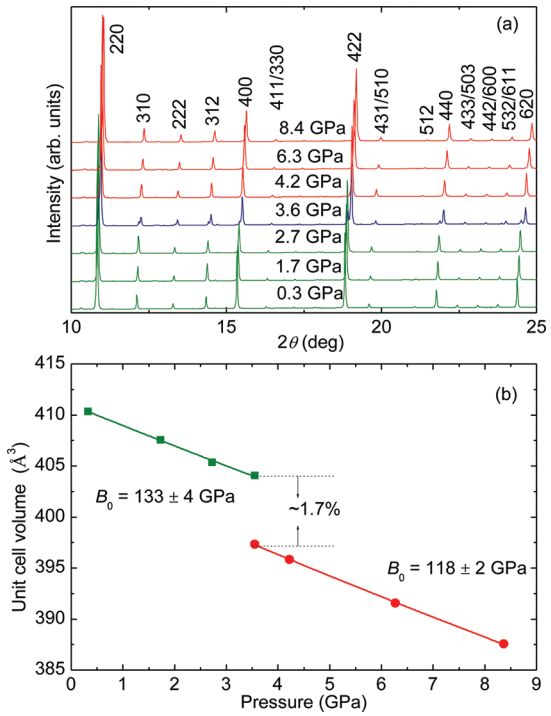

Figure 2. Pressure dependence of (a) SXRD patterns and (b) unit-cell volume for $LaCu_3Fe_4O_{12}$. The solid lines in (b) show the fitting results obtained using the isothermal Birch−Murnaghan equation of state.

confirms that the compound is crystallized with the charge formula $LaCu^{3+}{}_3Fe^{3+}{}_4O_{12}$, which is that of the low-temperature phase.[11] When the pressure is increased to 3.6 GPa, additional diffraction peaks appear and two cubic phases coexist. Above that pressure, the low-pressure phase disappears and the high-pressure phase is stable up to 8.4 GPa, which is the maximum pressure used in this study. The refined structure parameters of phases at representative low pressure (2.7 GPa) and high pressure (4.2 GPa) are listed in Table 1. Note that the high-pressure phase is isostructural to the low-pressure one.

As shown by the pressure dependence of unit-cell volume (Figure 2b), this isostructural phase transition is associated with a roughly 1.7% volume contraction, revealing the first-order nature of the transition. The pressure dependence of cell volume (V) could be well fitted to an isothermal Birch−Murnaghan equation of state,

$$p(V) = 1.5B_0[(V_0/V)^{7/3} - (V_0/V)^{5/3}] \times \{1 + 0.75(B_0' - 4)[(V_0/V)^{2/3} - 1]\} \quad (1)$$

where B_0 and B_0' are the bulk modulus and its pressure derivative, respectively.[15,16] B_0' is fixed to be 4, which is a typical value for elastic lattices. The B_0 obtained for the low-pressure and high-pressure phases are respectively 133 ± 4 and 118 ± 2 GPa. When pressure induces a structural phase transition, the high-pressure phase usually has a larger B_0 than the low-pressure phase. The B_0 of the high-pressure phase of $LaCu_3Fe_4O_{12}$, however, is about 11% smaller than that of the low-pressure phase. Such unusual softening has been seen in crystalline gallium[17] and a few other perovskite-structure

dx.doi.org/10.1021/cm301267e | Chem. Mater. 2012, 24, 2235−2239

Table 1. Refined Structure Parameters and Selected Bond Lengths of the $LaCu_3Fe_4O_{12}$ ($Z = 2$) Phases at Low Pressure (2.7 GPa) and High Pressure (4.2 GPa)[a]

pressure (GPa)	2.7	4.2
space group	$Im\bar{3}$	$Im\bar{3}$
a (Å)	7.4012(1)	7.3428(1)
V (Å^3)	405.41(2)	395.91(2)
U (100 × Å^2) for La	1.75(8)	1.34(8)
U (100 × Å^2) for Cu	2.73(7)	2.96(9)
U (100 × Å^2) for Fe	1.34(6)	1.03(8)
x for O	0.3211(5)	0.3133(6)
y for O	0.1695(6)	0.1744(7)
U (100 × Å^2) for O	0.03(1)	0.04(3)
Cu−O (Å) in CuO_4	1.824(4)	1.876(4)
Fe−O (Å) in FeO_6	2.014(1)	1.973(2)
R_{wp} (%)	4.45	5.43
R_p (%)	2.66	3.12

[a]Numbers in parentheses are standard deviations of the last significant digit. U is the isotropic thermal parameter. R_{wp} and R_p are agreement indices for the structure refinements by the Rietveld method.

materials[18−21] and is attributed to a significant change in electronic structure under high pressure. During this isostructural phase transition, indeed, the Cu−O bond length in the A-site square unit also abruptly increases whereas the Fe−O bond length decreases (see Table 1). The results strongly suggest a decrease in the valence state of Cu and an increase in the valence state of Fe. Thus, pressure appears to induce the same intersite charge transfer between the A-site Cu and B-site Fe that heating does.

The Mössbauer spectra provide convincing evidence for the changes of Fe charge and magnetic state under pressure. As shown in Figure 3, the Mössbauer spectra observed at 0.5 and 1.3 GPa are essentially the same as the spectra of the $LaCu^{3+}{}_3Fe^{3+}{}_4O_{12}$ phase.[11] The isomer shift (IS) ≈ 0.33 mm s^{-1} and the hyperfine field (HF) ≈ 46 T indicate that Fe^{3+} with a high-spin configuration orders antiferromagnetically (Figure 4a, b). When pressure increases to 1.9 GPa, a minor nonmagnetic singlet that coexists with the major sextuplet is seen. With further increasing pressure, the relative abundance of the sextuplet decreases and the singlet becomes dominant (Figure 4c). The singlet signals with IS ≈ 0.18 mm s^{-1} at high pressures are quite similar to the singlet signal seen in the spectrum of the high-temperature $LaCu^{2+}{}_3Fe^{3.75+}{}_4O_{12}$.[11] Note that the IS and HF of the low-pressure phase are almost constant and the IS of the high-pressure phase also does not change with changing pressure. The transition is thus characterized by the first-order-type change in the relative abundance of the phases. The results clearly indicate that applying pressure causes the change of Fe from antiferromagnetically ordered Fe^{3+} to paramagnetic $Fe^{3.75+}$. Although the two-phase coexistence region is slightly different from that observed in SXRD experiments, the transition from the low-pressure phase to the high-pressure one occurs around 3 GPa. This difference might originate from the difference in the experimental conditions.

It is therefore clear that pressure induces the intersite charge transfer at room temperature between the A-site Cu and B-site Fe ions. The insulator-to-metal transition observed in the resistivity measurement increasingly higher pressures is also consistent with the charge state transition, as shown in Figure 5. Because the electric transport properties of the A-site-ordered double-perovskite-structure materials are mainly governed by

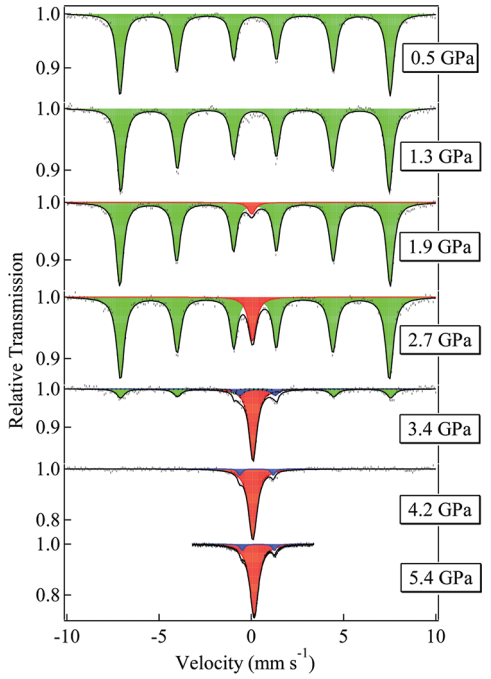

Figure 3. $LaCu_3Fe_4O_{12}$ Mössbauer spectra measured at different pressures. The dots show experimental data, and the green, red, and blue areas respectively show the sextuplet due to Fe^{3+} ions, the singlet due to $Fe^{3.75+}$ ions, and the doublet due to Fe^{3+} ions. The small Fe^{3+} doublet signals originate from a small amount of Fe ions at the A site.

the nature of the BO_6 octahedra, the antiferromagnetically coupled Fe^{3+} with high-spin configuration makes the low-pressure $LaCu^{3+}{}_3Fe^{3+}{}_4O_{12}$ phase being a Mott insulator. During the charge transfer, however, the resistivity decreases by about 4 orders of magnitude due to the formation of mixed valence state at the B site in the high-pressure $LaCu^{2+}{}_3Fe^{3.75+}{}_4O_{12}$ paramagnetic phase.

These results also imply that moderate pressure (about 3 GPa) reduces the charge-transfer transition temperature of $LaCu_3Fe_4O_{12}$ from 393 to 298 K (room temperature). This is similar to what occurs in the $BiNiO_3$ perovskite, where pressure induces the charge-transfer transition from $Bi^{3+}{}_{0.5}Bi^{5+}{}_{0.5}Ni^{2+}O_3$ to $Bi^{3+}Ni^{3+}O_3$ at room temperature.[22] Because the charge-transfer transition in the pressure−temperature phase diagram for $BiNiO_3$ has a negative dT_{CT}/dp slope, applying pressure decreases the charge-transfer transition temperature.[23] In the $LaCu_3Fe_4O_{12}$ A-site-ordered double perovskite, the unusual high-valence $Fe^{3.75+}$ state at the B site is stabilized at high temperature and high pressure while the unusual Cu^{3+} state at the square-planar A site is stable at low temperature and low pressure. Because the energy levels of the high $Fe^{3.75+}$ and Cu^{3+} states are comparable, a small external stimulus changes the energy balance between the states. We thus see the transition between the two states as the intersite charge-transfer transition in $LaCu_3Fe_4O_{12}$ either by changing pressure at ambient temperature or by changing temperature at ambient pressure. It is also important that such an intersite charge transfer occurs in the A-site-ordered double-perovskite-structure oxides in which both the A- and B-site transition-metal cations accept the transferred charge.

Note here that the intersite charge-transfer transition temperature of another A-site-ordered double-perovskite-structure oxide $BiCu_3Fe_4O_{12}$ (428 K) is higher than that of $LaCu_3Fe_4O_{12}$ (393 K).[24] The lattice constant of $BiCu_3Fe_4O_{12}$ is

dx.doi.org/10.1021/cm301267e | Chem. Mater. 2012, 24, 2235−2239

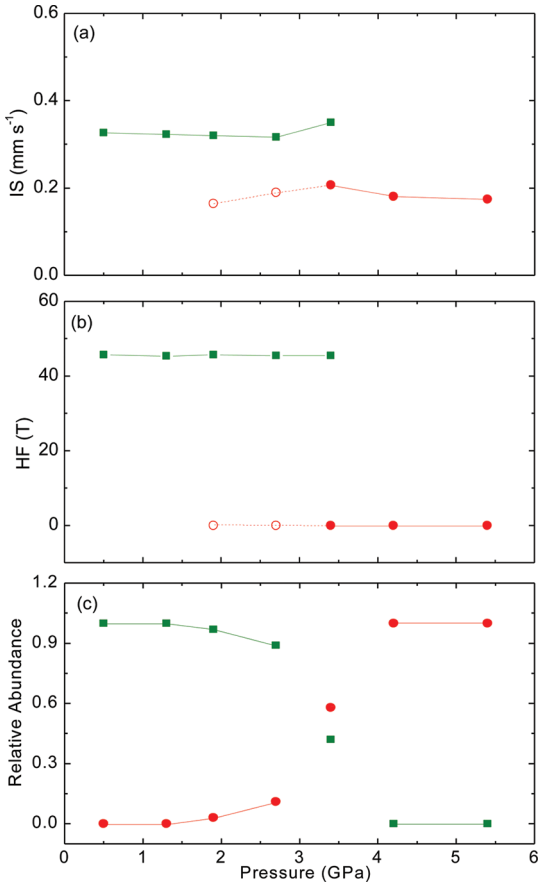

Figure 4. Pressure dependence of (a) isomer shift (IS), (b) hyperfine field (HF), and (c) relative abundance of the $LaCu_3Fe_4O_{12}$ Mössbauer spectra. The squares and circles present the sextuplet Fe^{3+} ions and the singlet $Fe^{3.75+}$ ions, respectively.

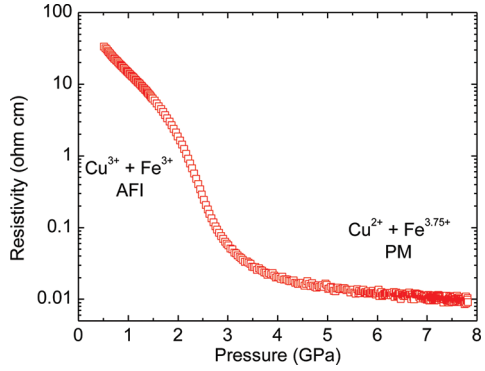

Figure 5. Pressure dependence of $LaCu_3Fe_4O_{12}$ resistivity at room temperature. AFI = antiferromagnetic insulator; PM = paramagnetic metal.

7.43322 Å at room temperature, which is larger than that of $LaCu_3Fe_4O_{12}$ (7.43283 Å),[24] and thus the charge-transfer transition temperature of the A-site-ordered double-perovskite-structure oxides decreases with decreasing volume. It implies that the charge-transfer transition temperature is reduced not only by physical pressure but also by the chemical pressure due to cation substitution. Reducing the unit-cell volume of $A'Cu_3Fe_4O_{12}$ in either a physical or chemical way thus stabilizes Cu^{2+} and $Fe^{3.75+}$ at the A and B sites and decease the intersite charge-transfer transition temperature.

4. CONCLUSIONS

We found a pressure-induced intersite charge transfer at room temperature between the A-site Cu and B-site Fe in the A-site-ordered double-perovskite-structure oxide $LaCu_3Fe_4O_{12}$. Synchrotron X-ray diffraction, Mössbauer spectroscopy, and resistivity measurements under high pressure revealed that the first-order charge-transfer transition from low-pressure $LaCu^{3+}{}_3Fe^{3+}{}_4O_{12}$ to high-pressure $LaCu^{2+}{}_3Fe^{3.75+}{}_4O_{12}$ is accompanied by significant volume reduction with unusual softening in bulk modulus and a change from an antiferromagnetic-and-insulating state to a paramagnetic-and-metallic state. The intersite charge-transfer transition in $LaCu_3Fe_4O_{12}$ is induced either by changing pressure at ambient temperature or by changing temperature at ambient pressure. Besides, the intersite charge transfer is caused by not only physical pressure but also chemical pressure by substituting cations at the A′ site. Reducing the unit-cell volume stabilizes the unusual high-valence $Fe^{3.75+}$ state at the B sites in the A-site-ordered double-perovskite-structure oxides.

AUTHOR INFORMATION

Corresponding Author

*E-mail: shimak@scl.kyoto-u.ac.jp (Y.S.).

Author Contributions

Y.W.L., T.K., T.S., and Y.S. designed the study. All authors contributed the sample synthesis and property measurements. The manuscript was written through contributions of all authors. All authors have given approval to the final version of the manuscript.

Notes

The authors declare no competing financial interest.

ACKNOWLEDGMENTS

We thank K. Oka, T. Tohyama, M. Azuma, A. Machida, and D. Kawana for help in the high-pressure experiments. We also thank N. Hayashi for helpful discussion on the Mössbauer experiments. The synchrotron radiation experiments were performed at SPring-8 with the approval of the Japan Synchrotron Radiation Research Institute. This work was partially supported by Grants-in-Aid for Scientific Research (Grants 19GS0207, 18350097, and 22740227), by the Joint Project of Chemical Synthesis Core Research Institutions, and by Global COE Program (B09) from the Ministry of Education, Culture, Sports, Science and Technology of Japan. The work was also supported by the CREST program of the Japan Science and Technology Agency. The Mössbauer experiments by T.K. and Y.N. were supported by the Strategic Research Base Development Program for Private Universities subsidized by MEXT (Grant S0901022). Y.W.L. was supported by the 100 Talents Project of the Chinese Academy of Sciences (Grant Y1k5019x51), and C.Q.J. was supported by the National Natural Science Foundation of China (Grant 91122035).

REFERENCES

(1) Vasil'ev, A. N.; Volkova, O. S. *Low Temp. Phys.* **2007**, *33*, 895.
(2) Shimakawa, Y. *Inorg. Chem.* **2008**, *47*, 8562.
(3) Homes, C. C.; Vogt, T.; Shapiro, S. M.; Wakimoto, S.; Ramirez, A. *Science* **2001**, *293*, 673.
(4) Prodi, A.; Gilioli, E.; Gauzzi, A.; Licci, F.; Marezio, M.; Bolzoni, F.; Huang, Q.; Santoro, A.; Lynn, J. W. *Nat. Mater.* **2004**, *3*, 48.

(5) Imamura, N.; Karppinen, M.; Motohashi, T.; Fu, D.; Itoh, M.; Yamauchi, H. *J. Am. Chem. Soc.* **2008**, *130*, 14948.
(6) Zeng, Z.; Greenblatt, M.; Subramanian, M. A.; Croft, M. *Phys. Rev. Lett.* **1999**, *82*, 3164.
(7) Weht, R; Pickett, W. E. *Phys. Rev. B* **2001**, *65*, 014415.
(8) Alonso, J. A.; Sánchez-Benítez, J.; De Andrés, A.; Martínez-Lope, M. J.; Casais, M. T.; Martínez, J. L. *Appl. Phys. Lett.* **2003**, *83*, 2623.
(9) Liu, X. -J.; Xiang, H. -P.; Cai, P.; Hao, X. -F.; Wu, Z. -J.; Meng, J. *J. Mater. Chem.* **2006**, *16*, 4243.
(10) Takata, K.; Yamada, I.; Azuma, M.; Takano, M.; Shimakawa, Y. *Phys. Rev. B* **2007**, *76*, 024429.
(11) Long, Y. W.; Hayashi, N.; Saito, T.; Azuma, M.; Muranaka, S.; Shimakawa, Y. *Nature* **2009**, *458*, 60.
(12) Chen, W.; Long, Y. W.; Saito, T.; Attfield, J. P.; Shimakawa, Y. *J. Mater. Chem.* **2010**, *20*, 7282.
(13) Mao, H. K.; Xu, J.; Bell, P. M. *J. Geophys. Res.* **1986**, *91*, 4673.
(14) Larson, A. C.; von Dreele, R. B. *General Structure Analysis System (GSAS)*; Report No. LAUR 86−748 ; Los Alamos National Laboratory: Los Alamos, NM, 1994.
(15) Birch, F. *Phys. Rev.* **1947**, *71*, 809.
(16) Murnaghan, F. D. *Proc. Natl. Acad. Sci. U.S.A.* **1944**, *30* (9), 244.
(17) Lyapin, A. G.; Gromnitskaya, E. L.; Yagafarov, O. F.; Stal'gorova, O. V.; Brazhkin, V. V. *J. Exp. Theor. Phys.* **2008**, *107*, 818.
(18) Zhou, J. S.; Yan, J. Q.; Goodenough, J. B. *Phys. Rev. B* **2005**, *71*, 220103(R).
(19) Vogt, T.; Hriljac, J. A.; Hyatt, N. C.; Woodward, P. *Phys. Rev. B* **2003**, *67*, 140401.
(20) Zhou, J. S.; Goodenough, J. B.; Dabrowski, B. *Phys. Rev. B* **2004**, *70*, 081102.
(21) Zhou, J. S.; Jin, C. Q.; Long, Y. W.; Yang, L. X.; Goodenough, J. B. *Phys. Rev. Lett.* **2006**, *96*, 046408.
(22) Azuma, M.; Carlsson, S.; Rodgers, J.; Tucker, M. G.; Tsujimoto, M.; Ishiwata, S.; Isoda, S.; Shimakawa, Y.; Takano, M.; Attfield, J. P. *J. Am. Chem. Soc.* **2007**, *129*, 14433.
(23) Azuma, M.; Chen, W.; Seki, H.; Czapski, M.; Olga, S.; Oka, K.; Mizumaki, M.; Watanuki, T.; Ishimatsu, N.; Kawamura, N.; Ishiwata, S.; Tucker, M. G.; Shimakawa, Y.; Attfield, J. P. *Nature Commun.* **2011**, *2*, 347.
(24) Long, Y. W.; Saito, T.; Tohyama, T.; Oka, K.; Azuma, M.; Shimakawa, Y. *Inorg. Chem.* **2009**, *48*, 8489.